JOURNAL OF MATERIALS SCIENCE 32 (1997) 5177–5184

Synthesis characterization and hydrogen absorption studies of the composite materials La_2Mg_{17}–x wt% $LaNi_5$

K. PAL (NEE DUTTA)
Machine Intelligence Unit, Indian Statistical Institute, 203 B.T. Road, Calcutta 700 035, India

The composite materials La_2Mg_{17}–x wt% $LaNi_5$ have been synthesized with various values of x, and the hydrogenation behaviour of these materials has been extensively studied. The as-synthesized materials were activated by heating the materials at about 360 ± 10 °C temperature under a hydrogen pressure of 33 $kg\,cm^{-2}$ for nearly 6 h. The maximum hydrogen storage capacity was found to be 5.3 wt% for the composite material La_2Mg_{17}–10 wt% $LaNi_5$ at 400 ± 10 °C temperature. This is one of the very highest storage capacities known so far. The initial rate of hydrogen absorption of La_2Mg_{17}–10 wt% $LaNi_5$ was found to be 20 $cm^3\,g^{-1}\,min^{-1}$ (at 400 ± 10 °C temperature). In order to elucidate the influence of $LaNi_5$ addition, which significantly accelerated the hydriding rate and hydrogen storage capacity of La_2Mg_{17}, structural–microstructural characterization and chemical analysis of the composite materials employing X-ray diffraction, scanning electron microscopy and energy dispersive analysis of X-rays techniques have been carried out.

1. Introduction

For harnessing hydrogen as an alternative fuel, one of the crucial aspects is to develop efficient hydrogen-storage systems. It has been found that some judicially combined composite materials perform differently and often more efficiently than the constituent materials themselves. The simple composite concept is an extremely useful and, in some aspect, an altogether new way of thinking about the development and application of hydrogen-storage materials. Although the ever increasing demand and application of composites claim continued improvement in the synthesis of materials, in the field of hydrogen storage, the development of composite materials has entered the arena only lately, in the last few years. So far, investigation of hydrogen-storage materials has centred on individual intermetallics, capable of reversible hydrogenation behaviour. Magnesium and magnesium-based alloys are considered superior to other storage materials, because of higher hydrogen density, and lower weight and cost [1–4]. The magnesium-containing systems such as La_2Mg_{17} and $LaMg_{12}$ have suitable thermodynamic attributes for hydrogen storage. However, a significant disadvantage of these materials is the very slow absorption–desorption kinetics – this is about ten times slower than that of the well-known hydrogen-storage material, $LaNi_5$ [5]. Recently, there have been some investigations which suggest that composite-like materials may possess better hydriding characteristics [6–10]. Such studies are rather sparse and in order to test the viability of composite materials for storing hydrogen, further investigations are required.

Keeping in mind the fact that composite materials may possess properties better than those exhibited by both of its ingredients, we have attempted to synthesize La_2Mg_{17}–x wt% $LaNi_5$ (the former is a high storage capacity but slow kinetics material and latter is a low storage-capacity but fast kinetics material) for various values of x, with the expectation of achieving a high-capacity and fast kinetics composite material.

2. Experimental procedure

At first the native ingredient La_2Mg_{17} was synthesized through a solid-state diffusion process, by taking stoichiometric quantities of highly pure constituent elements lanthanum (99.9%) and magnesium (99.99%) pressed in a pellet form. A somewhat new synthesis route aimed at avoiding evaporation/sublimation of the low-melting component, magnesium, was adopted. This consisted in encapsulation of the subliming component, magnesium, by lanthanum from all sides. The reasons behind this are that the melting (boiling) point of magnesium is lower than that of lanthanum, and magnesium transforms directly from solid to the vapour state. The process of pellet formation was as follows. Pellets of magnesium and lanthanum with diameters d and D (such that $d < D$) respectively, were prepared. The magnesium pellet was placed on the middle of a lanthanum Pellet. Then the area surrounding the magnesium pellet and its upper surface were covered with lanthanum flux, as shown in Fig. 1. This configuration was then pressed to achieve magnesium encapsulation by the lanthanum matrix. The pellet sizes were optimized so that

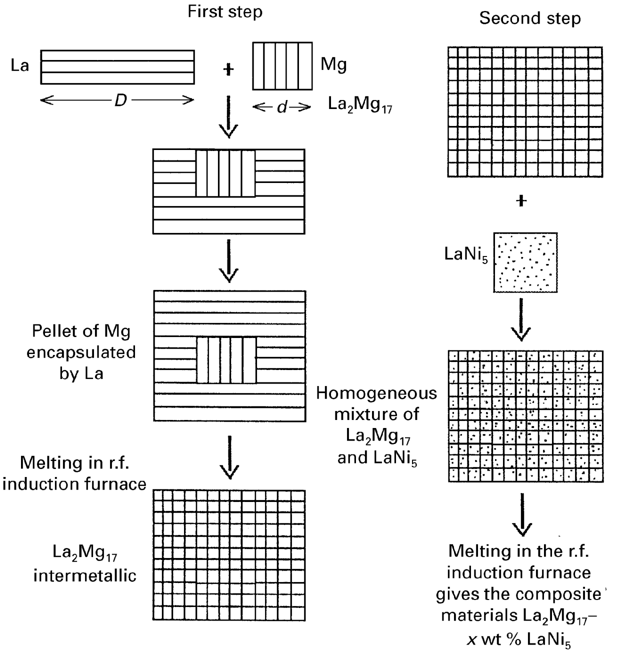

Figure 1 Schematic diagram of the preparation of the pellet.

they can carry appropriate quantities of lanthanum and magnesium in a compact way. The superiority of this method is that, when the pellets are melted, practically no magnesium escapes. This leads to the correct stoichiometric formation of the intermetallic compound La_2Mg_{17}. The pellets were melted in a prebaked quartz tube under an argon atmosphere (1 kg cm^{-2} pressure) with the help of the radiofrequency (r.f.) induction furnace (12 kW). To avoid contamination of the flux ingredients, particularly magnesium, water was circulated in the outer jacket. Then the as-synthesized intermetallic, which presumably possesses very nearly the envisaged stoichiometry, was quenched to room temperature. In the next step, the composite materials La_2Mg_{17}–x wt % $LaNi_5$ with $x = 5$, 10, 20, 30 and 40 were synthesized. The pellets of homogeneous mixture of La_2Mg_{17} and $LaNi_5$ in the proper stoichiometric ratios are melted in the r.f. induction furnace under an argon atmosphere with the same experimental set up as before.

The hydriding characteristics of the composite materials La_2Mg_{17}–x wt % $LaNi_5$ (when $x = 5$, 10, 20, 30 and 40) were evaluated through the measurement of pressure–composition isotherms and kinetic curves of hydrogenation. These measurements were monitored by a volumetric method after preliminary out-gassing of the reactor vessel using the set up as described elsewhere [11] . At first, the as-synthesized materials were activated by heating the materials at about $360 \pm 10\,^{\circ}$C under a hydrogen atmosphere (33 kg cm^{-2}). Heating was continued for nearly 6 h under the same hydrogen atmosphere. The quantities of absorbed hydrogen as a function of time were measured volumetrically by recording the variation in the hydrogen pressure of the hydrogen reactor with time.

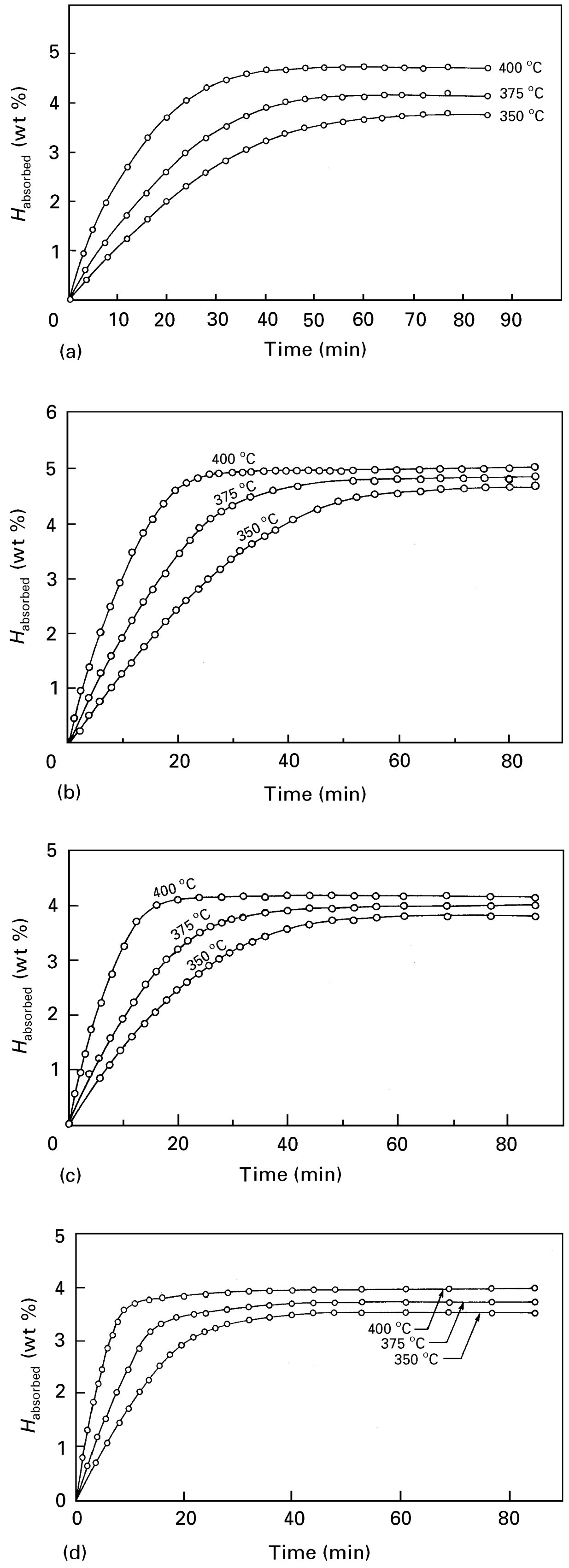

Figure 2 Kinetic curves of hydrogen absorption at different temperatures and at a pressure of 4 kg cm^{-2} for La_2Mg_{17}–x wt % $LaNi_5$ for (a) $x = 5$, (b) $x = 10$, (c) $x = 20$ and (d) $x = 40$.

The structural characterization of the composite materials was carried out through X-ray diffraction (XRD). A Philips wide-angle X-ray powder diffractometer PW-1710 was used for this purpose. The scanning electron micrographs of the above-mentioned composite materials were obtained on the same sample, on which the XRD analysis was performed. Transverse sections of the specimens were cut and polished by standard metallographic techniques and the compositions of the as-synthesized composite materials were determined by PV-9900 equipment for energy dispersive analysis of X-rays (EDAX) attached to a Philips EM-CM-12 electron microscope.

3. Results and discussion

3.1. Determination of the hydriding characteristics of La_2Mg_{17}–x wt% $LaNi_5$

The hydrogenation rates of the as-synthesized composite materials La_2Mg_{17}–x wt % $LaNi_5$ were measured at a temperature ranging from 350–400 °C. Fig. 2a–d show the kinetic curves of hydrogen absorption at different temperatures and at a pressure of 4 kg cm^{-2} for La_2Mg_{17}–x wt % $LaNi_5$ with $x = 5$, 10, 20 and 40, respectively. These results indicate that hydrogen absorption is strongly affected by temperature. It has been evident that addition of $LaNi_5$ in La_2Mg_{17} accelerated the hydriding rate by about three to four times in comparison to La_2Mg_{17} alone. At the beginning, the uptake of hydrogen is nearly linear with time and decreased with longer time. The rate of hydriding can be obtained from the slope of the curves. We observed the highest hydrogenation rate for a material hydrided at the highest pressure and temperature.

The curves depicted in Fig. 2a–d suggest that the highest hydrogen-storage capacity corresponds to the composite material La_2Mg_{17}–10 wt % $LaNi_5$. In order to verify this and to estimate the hydrogen-storage capacity, we have evaluated the pressure–composition–temperature (P–C–T) relationship of the composite materials La_2Mg_{17}–x wt % $LaNi_5$ for various values of x. The experiments to obtain P–C–T isotherms of the composite materials were performed on the same sample on which the hydriding kinetics measurements were carried out. P–C–T measurements show the relationship between the hydrogen pressure and composition for a particular temperature. From P–C–T measurements, (i) the solid solubility of hydrogen in the metallic lattice, (ii) the range of composition at constant pressure, (iii) the overall hydrogen content, and (iv) the equilibrium hydrogen pressure as a function of the temperature can be deduced. Fig. 3a–d shows the pressure–composition hydrogen absorption isotherms at three different temperatures, 350, 375 and 400 °C, for the composite materials La_2Mg_{17}–x wt % $LaNi_5$ with $x = 5$, 10, 20 and 40, respectively. In all cases, clear-cut plateaux were observed. As seen from the figures, P–C isotherms vary considerably according to the amount of $LaNi_5$ added to La_2Mg_{17}. With increase of temperature there is an increase of the plateau pressure of the composite materials. The maximum hydrogen-storage capacity of this material is 5.3 wt % for $x = 10$ (at 400 ± 10 °C). We observed that the crushed sample of the composite material La_2Mg_{17}–x wt % $LaNi_5$ (with particle size 1 mm) which was degassed for 12–16 h (in several steps) reacts rapidly with hydrogen at a pressure of 33 kg cm^{-2} to yield this higher storage capacity. After four hydrogenation–dehydrogenation cycles, the powder was found to be very active.

Plots of the maximum hydrogen content as a function of $LaNi_5$ content at different temperatures are shown in Fig. 4 for the composite materials La_2Mg_{17}–x wt % $LaNi_5$.

It has been found that the hydriding–dehydriding behaviour in a metal hydrogen system is affected by different factors, including alloy compositions, hydriding and dehydriding temperature and pressure. We also noticed that after ten hydrogenation–dehydrogenation cycles, the sample becomes a fine particle-size powder. The temperature at which hydrogen absorption took place becomes lower with increasing $LaNi_5$ content in the composite materials.

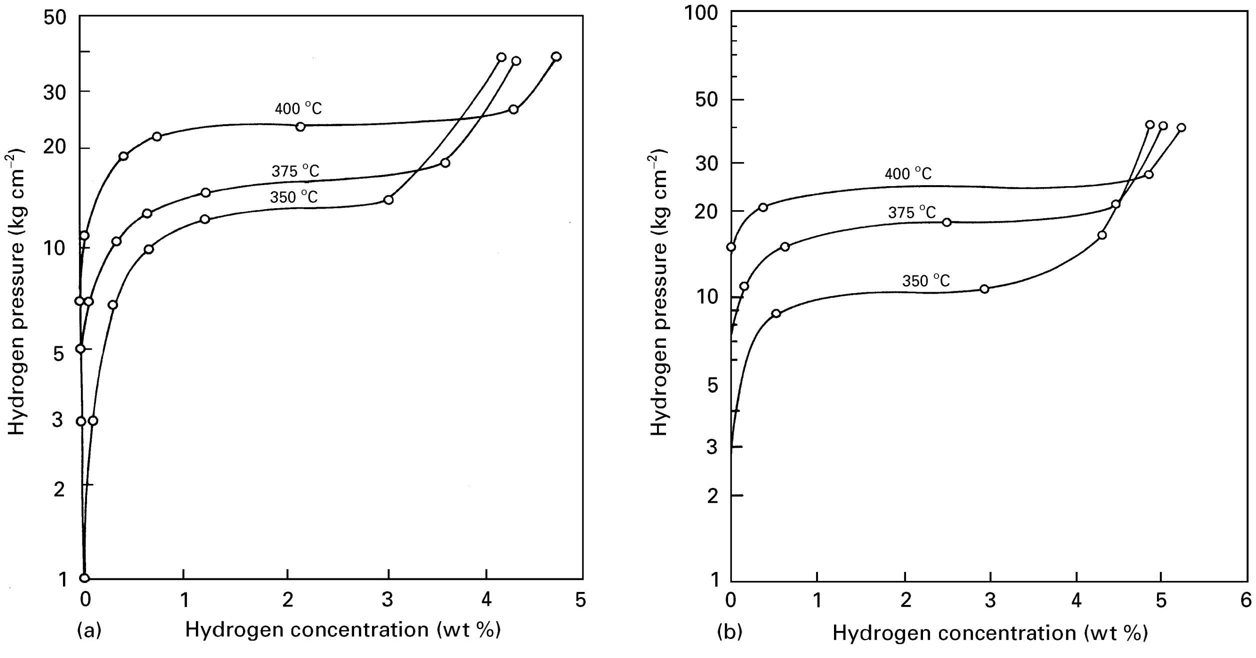

Figure 3 Pressure–composition isotherms of the composite materials La_2Mg_{17}–x wt % $LaNi_5$ with (a) $x = 5$, (b) $x = 10$, (c) $x = 20$ and (d) $x = 40$.

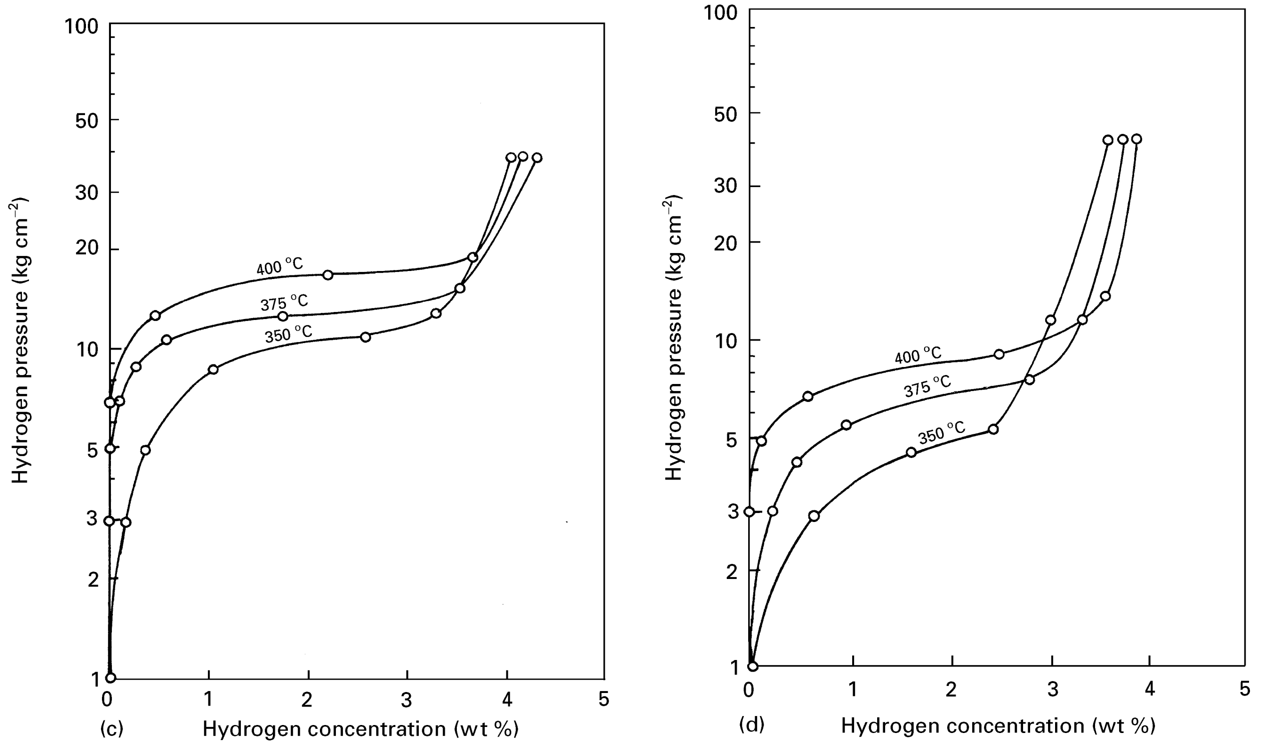

Figure 3 (Continued)

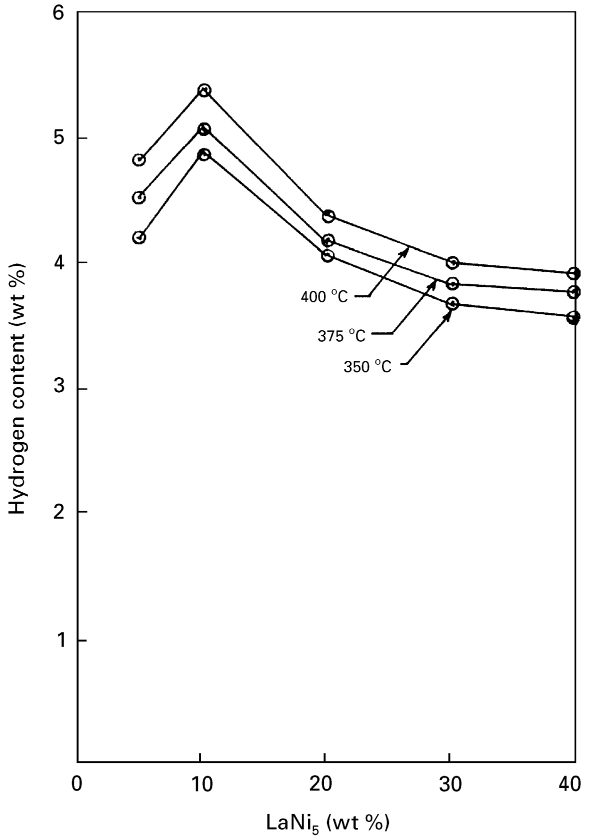

Figure 4 Maximum hydrogen content as a function of the content of $LaNi_5$ for the composite materials La_2Mg_{17}–x wt % $LaNi_5$ for ($x = 5$, 10, 20, 30 and 40) at different temperatures..

Assessment of the potential of intermetallic hydrides and many binary, ternary and more complex alloy hydrides as reversible hydrogen-storage materials, requires the prediction of a number of their properties, of which thermodynamic characteristics are the most important. It is known that the pressure–composition isotherm measurements can be indirectly used for characterization of thermal effects. The enthalpies and entropies of hydride formation and dissociation can be determined from the absorption and desorption isotherms of the composite materials from Van't Hoff plots. Fig. 5a–d show the dependence of dissociation pressure on the reciprocal of temperature T, for the composite materials La_2Mg_{17}–x wt % $LaNi_5$ with (a) $x = 5$, (b) $x = 10$, (c) $x = 30$ and (d) $x = 40$, respectively; where the value of pressure at the centre of the plateau region has been taken as the dissociation pressure. From the linear relation between $\ln P$ and $1/T$, the relative partial molar enthalpy ΔH_H and entropy ΔS_H can be determined for these composite materials by using the Van't Hoff equation

$$ln(p) = \frac{\Delta H_H}{RT} - \frac{\Delta S_H}{R} \qquad (1)$$

3.2. Structural characterization – XRD, SEM and EDAX explorations

In order to understand the influence of $LaNi_5$ addition, which significantly accelerated the hydriding rate and hydrogen-storage capacity of La_2Mg_{17}, the structural, microstructural and chemical analysis of the composite materials employing the X-ray diffraction (XRD), scanning electron microscopy (SEM) and energy dispersive X-ray analysis (EDAX) techniques have been carried out.

The initial attempts to study structural characterization of the composite materials La_2Mg_{17}–x wt % $LaNi_5$ for $x = 5$, 10, 20, 30 and 40 were carried out

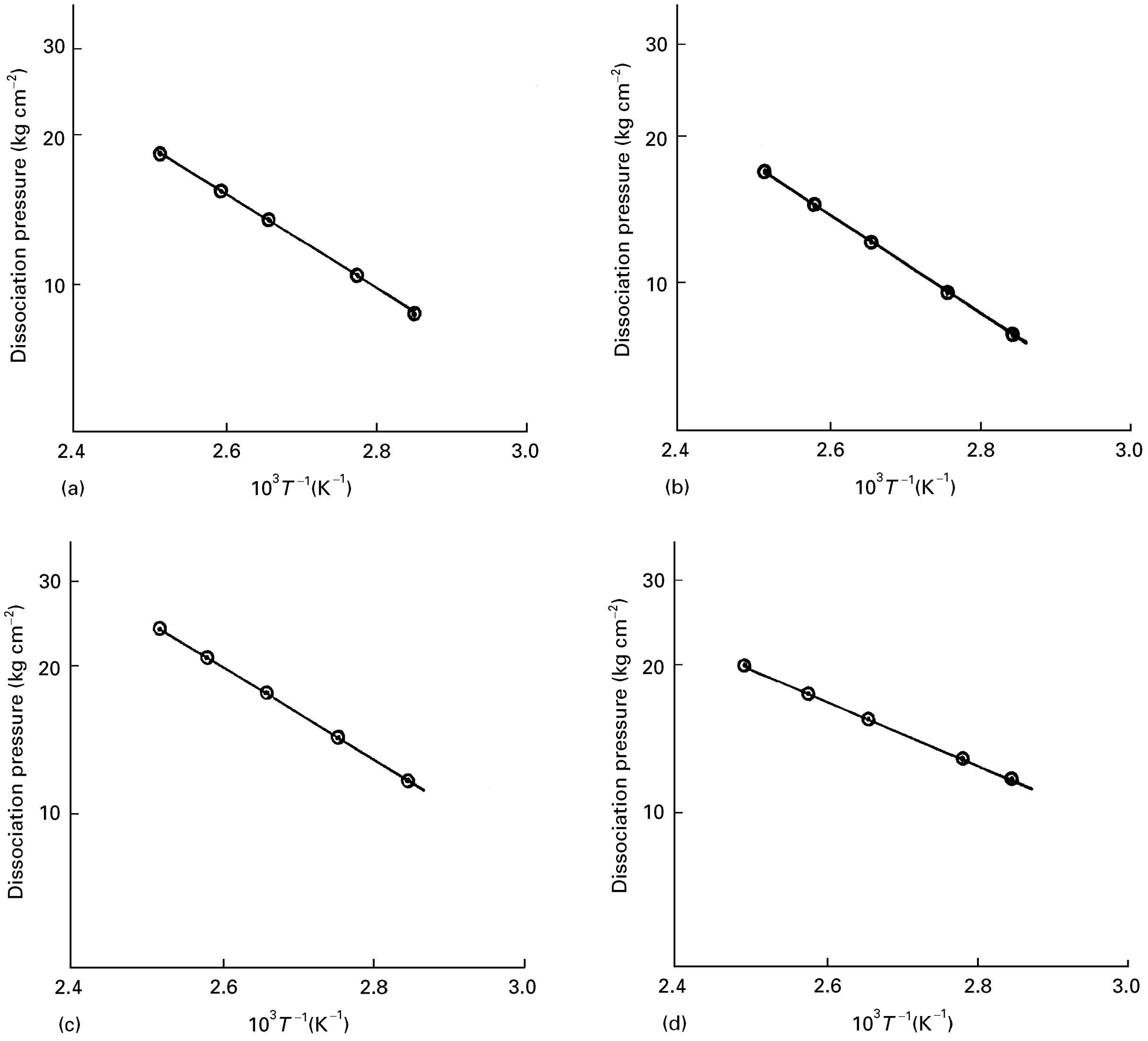

Figure 5 Van't Hoff plots for the composite materials La_2Mg_{17}–x wt % $LaNi_5$ for (a) $x = 5$, (b) $x = 10$, (c) $x = 30$ and (d) $x = 40$.

with the help of XRD. The XRD results of these composite materials revealed that the as-synthesized materials are multiphasic in nature. Fig. 6a–c show the representative XRD patterns of the as-synthesized composite materials La_2Mg_{17}–x wt % $LaNi_5$ for $x = 5$, 10 and 20, respectively. Different phases are marked on the figures. It is clear from these XRD patterns that although the dominant as-synthesized phase was of La_2Mg_{17}, some phases which were representative of $MgNi_2$, $LaNi_3$ and nickel appeared.

Ideally, in the investigation of the interaction of hydrogen with the composite materials, one should examine the surface of the material in atomic resolution, so that its morphology could be precisely defined. In addition, the chemical density of all surface compositions should be known so that the process of chemical reaction between hydrogen and intermetallics could be well understood.

Fig. 7a shows a representative SEM image, made through secondary electrons, of the as-synthesized composite material La_2Mg_{17}–10 wt % $LaNi_5$, showing the multiphasic nature of the material. Small grains and precipitate-like particles are observed on the large crystallites. The EDAX analyses confirmed that the larger crystallites are La_2Mg_{17}-rich, marked L, and small precipitate-like crystallites are nickel-rich, marked S, on the photograph. These nickel-rich particles are believed to be precipitates of $MgNi_2$, $LaNi_3$ and nickel phases. Fig. 8a shows the representative EDAX pattern of the as-prepared composite material La_2Mg_{17}–10 wt % $LaNi_5$, taken from the larger crystallites (indicated by L) of the above electron micrograph, whereas Fig. 8b shows the EDAX pattern from the smaller particles of the electron micrograph (indicated by S in the photograph). It is evident from these figures that the surface under consideration is nickel-rich, which may be the cause of the fast hydriding kinetics and large storage capacity of these materials. The presence of nickel, either embodied in $MgNi_2$, $LaNi_3$ or in the free form, presumably accelerated the hydrogen absorption–desorption, leading to the observed better hydriding characteristics of the composite materials. We can infer that an important parameter influencing hydrogenation–dehydrogenation is the surface nickel in contact with La_2Mg_{17} and other nickel-bearing phases. Free nickel was present for all values of x. It is known that nickel on the surface decreases the activation energy of

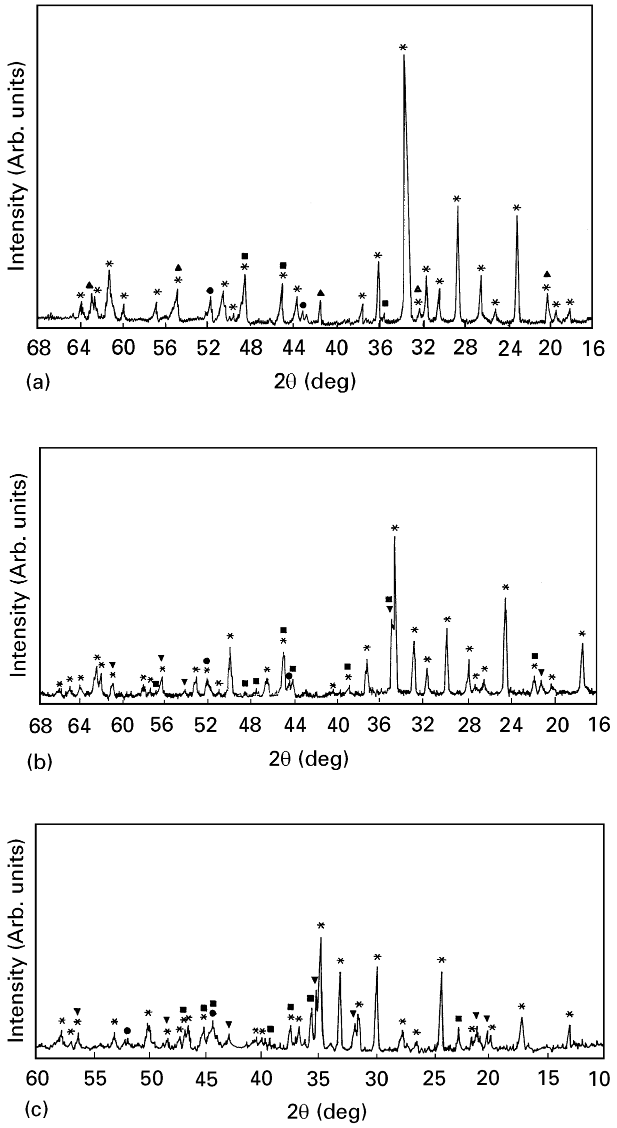

Figure 6 X-ray diffraction patterns of the as-synthesized composite materials La_2Mg_{17}–x wt % $LaNi_5$ for (a) $x = 5$, (b) $x = 10$, (c) $x = 20$ (*) La_2Mg_{17}, (▼) $LaNi_3$, (■) $MgNi_2$, (●) Ni.

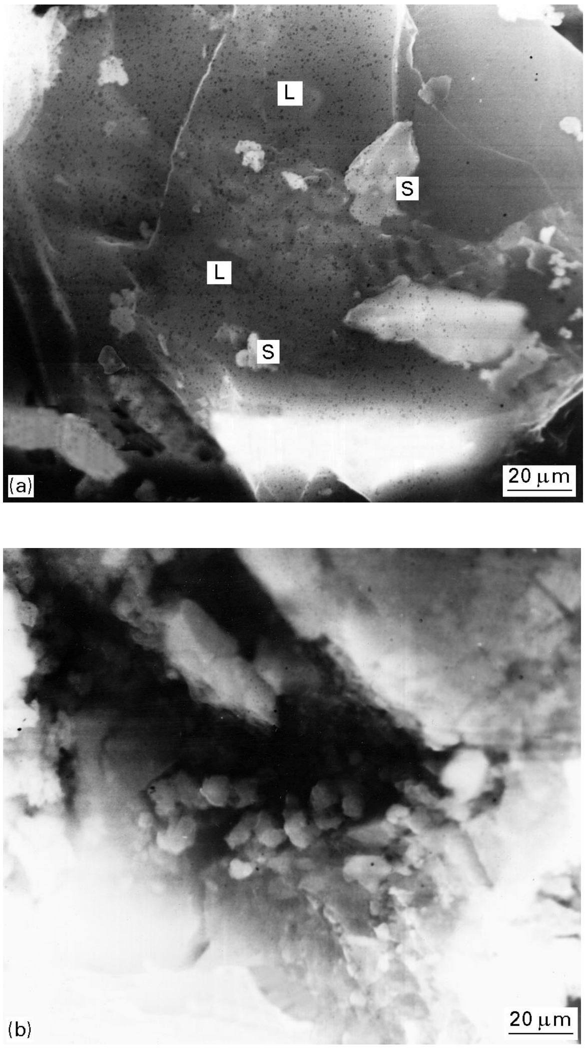

Figure 7 (*a*) A representative scanning secondary electron micrograph of the as-synthesized composite material La_2Mg_{17}–10 wt % $LaNi_5$ indicating the presence of two types of crystallites, large (L) and small (S) on the surface. (b) A representative scanning electron micrograph of the dehydrogenated composite material La_2Mg_{17}–10 wt % $LaNi_5$ indicating that the material converts into fine particle-size powder after ten hydrogenation–dehydrogenation cycles.

dissociation of hydrogen molecules. The hydriding rate and storage capacity appears to be dependent on the nickel-containing phases which form sites favourable to hydride nucleation and also serve as channels by which hydrogen would enter and come out of the main phase. The rapidity with which the composite materials absorb and desorb hydrogen seem to suggest that the additional phases, particularly those embodying nickel, may also affect the kinetics and play a crucial role in the acceleration of hydriding rates of the composite materials.

The difference in the hydriding characteristics of the composite materials for various values of x is considered to be due to the difference in the amounts and types of phases present in the materials. This is clear from the XRD patterns (see Fig. 6a–c), that with increasing values of x, the number of peaks of minority phases (such as $MgNi_2$, $LaNi_3$) increased. The large amount of these phases act as a barrier for hydrogen absorption and desorption, and this may be the reason that different storage characteristics of the composite materials La_2Mg_{17}–x wt % $LaNi_5$ were obtained for various values of x.

We propose the following reaction mechanism for the composite materials. Hydrogen molecules come into contact with the surface of the composite materials and dissociate ($H_2 \rightarrow H + H$) at the nickel particles which are present on the surface of the composites. Then the atomic hydrogen diffuses to interstitial positions of the main phase and thus becomes absorbed. Other nickel-containing minority phases (e.g. $MgNi_2$, $LaNi_3$) act as catalysts for hydrogen sorption. Thus, the optimum storage capacity of 5.3 wt % for La_2Mg_{17}–10 wt % $LaNi_5$ with very fast hydrogenation–dehydrogenation kinetics, appears appreciable. Therefore, it is clear that the initial rate of hydrogen absorption by the composite materials is controlled by surface chemisorption and the rate of chemisorption is closely related to the phases present on the surface, and to the surface area.

The representative scanning electron micrograph made through secondary electrons, of the partially

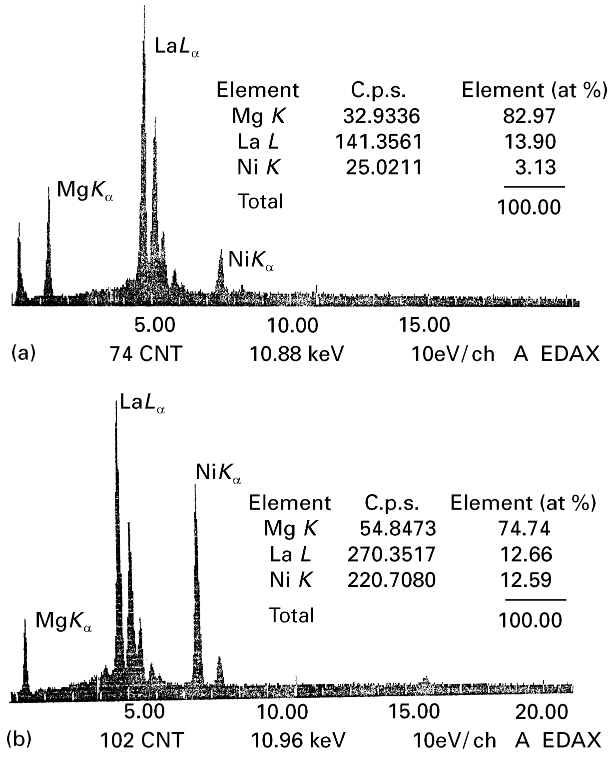

(a)

Element	C.p.s.	Element (at %)
Mg *K*	32.9336	82.97
La *L*	141.3561	13.90
Ni *K*	25.0211	3.13
Total		100.00

(b)

Element	C.p.s.	Element (at %)
Mg *K*	54.8473	74.74
La *L*	270.3517	12.66
Ni *K*	220.7080	12.59
Total		100.00

Figure 8 EDAX spectrum of the as-prepared composite material La_2Mg_{17}–10 wt % $LaNi_5$ taken from (a) a larger crystallite (L) and (b) a smaller crystallite (S) of Fig. 7a.

reacted surface (reaction between composite material and hydrogen) can be seen in Fig. 9a. Fig. 9b reflects that most of the surface becomes reacted with longer exposure of the material under hydrogen pressure and at high temperature. The total time for the reaction was about 2 h at high temperature (after several hydrogenation–dehydrogenation cycles). Because the particles of the activated sample were observed by scanning electron microscopy, to have irregular shapes, it is impossible to establish a simple relation between the variation in the reacting phases and reacted area. The surface studies of metal hydrides using scanning electron microscopic techniques indicate that surface compositions play a major role in the use of composite materials as hydrogen fuel-storage media. Fig. 7b is an illustrative SEM image of the dehydrogenated composite material La_2Mg_{17}–10 wt % $LaNi_5$ after ten hydrogenation–dehydrogenation cycles. It is clear from this secondary electron image that the material becomes fine particle-size powder after several hydrogenation–dehydrogenation cycles. In all cases, increase in the number of cycles produce more fracture and breakage of the material into small domains (up to a limit). Comparison of the surfaces of tha as-synthesized and dehydrogenated composite material La_2Mg_{17}–10 wt % $LaNi_5$ confirms that after several hydrogenation–dehydrogenation cycles, the surface becomes sponge-like.

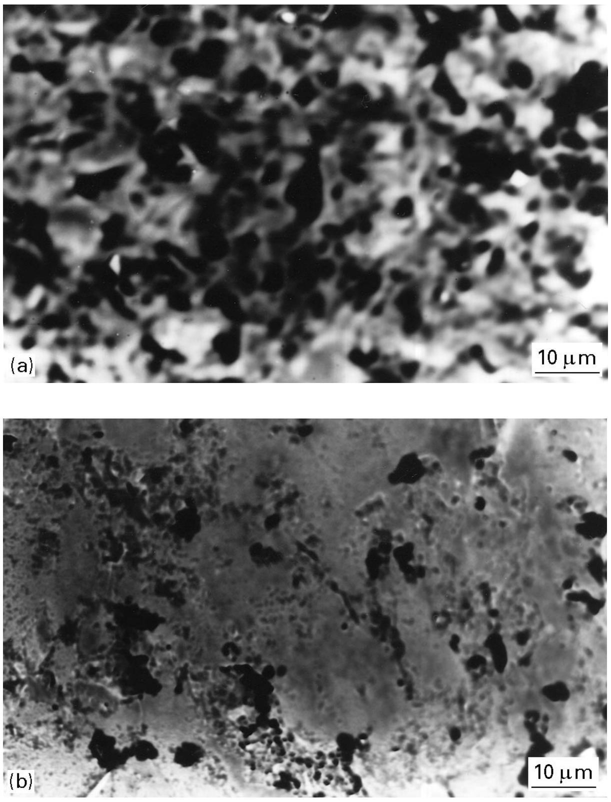

Figure 9 The representative scanning electron micrographs, made through secondary electrons of the hydrogenated composite material La_2Mg_{17}–10 wt % $LaNi_5$ (a) The partially reacted surface (reaction between composite material and hydrogen) can be seen. (b) After longer exposure of the material under hydrogen pressure and at high temperature, most of the surface becomes reacted.

4. Conclusion

Composite materials La_2Mg_{17}–x wt % $LaNi_5$ have been synthesized successfully for various values of x (x = 5, 10, 20, 30 and 40), and the hydriding behaviour of these new composite materials were studied. The initial rate of hydrogen absorption of La_2Mg_{17}–10 wt % $LaNi_5$ was found to be 20 cm^3 m^{-1} min^{-1} (at 400 ± 10 °C). The optimum storage capacity of 5.3 wt% with respect to pressure and composition was observed of La_2Mg_{17}–10 wt % $LaNi_5$ at 400 ± 10 °C. In contrast to the presently known high hydrogen-storage capacity of 3.8 wt% for Mg_2Ni, the present capacity of 5.3 wt% is higher by more than 39%. In order to understand the role of $LaNi_5$ in accelerating the hydriding–dehydriding behaviour of La_2Mg_{17}, investigations on structural–microstructural characteristics of the composite materials were carried out employing XRD, SEM and EDAX techniques. It was observed that hydriding rates and hydrogen-storage capacities are closely related to the microstructures and types of phases present in the materials. The increase in the hydrogenation rates appears to be produced by a catalytic effect of the minority phases $MgNi_2$ and $LaNi_3$, in addition to free nickel phase on the surface and bulk. In the present case, surface nickel initiated the chemisorption. The present results are suggestive of the fact that activation depends strongly on the surface structures of the as-synthesized composite materials.

Acknowledgements

I am grateful to the Department of Non-conventional Energy Sources, India and the Council of Scientific and Industrial Research, India for financial support.

I wish to thank Professor O. N. Srivastava, Department of Physics, Banaras Hindu University, Varanasi, India, for his interest in this work.

References

1. M. PEZAT, B. DARRIET and J. HAGENMULLER, *J. Less-Common Metals* **74** (1980) 427.
2. M. KHRUSSANOVA, M. TERZIEVA, P. PESHEV and K. PETROV, *Int. J. Hydrogen Energy* **9** (1985) 591.
3. P. SELVAM, B. VISWANATHAN, C. S. SWAMY and V. SRINIVASAN, *ibid.* **11** (1986) 169.
4. V. N. VERBETSKY and S. N. KLYAMKIN, *Izv. AN SSSR. Metally* **2** (1987) 209.
5. K. DUTTA and O. N. SRIVASTAVA, *Int, J. Hydrogen Energy* **18** (1993) 397.
6. E. E. EATON, G. E. OLSEN, H. SHEINBERG and W. A. STEYERT, *ibid.* **6** (1981) 609.
7. H. SUZUKI, Y. OSUMI, A. KATO, K. OGURO and M. NAKANE, *J. Chem. Soc. Jpn* **117** (1981) 1493.
8. H. ISHIKAWA, K. OGURO, A. KATO, H. SUZUKI and E. ISHII, *J. Less-Common Metals* **107** (1985) 105.
9. H. NAGAI, H. TOMIZAWA, T. OGASAWARA and K. SHOJI, *ibid.* **157** (1990) 15.
10. H. FUJII, S. ORIMO and K. YAMAMOTO, *ibid.* **175** (1991) 243.
11. K. DUTTA and O. N. SRIVASTAVA, *J. Mater. Sci.* **28** (1993) 3457.

Received 8 January 1996
and accepted 4 April 1997